Hindawi Publishing Corporation
Journal of Spectroscopy
Volume 2013, Article ID 346826, 16 pages
http://dx.doi.org/10.1155/2013/346826

Research Article

The Kinetics of Joined Action of Triplet-Triplet Annihilation and First-Order Decay of Molecules in T_1 State in the Case of Nondominant First-Order Process: The Kinetic Model in the Case of Spatially Periodic Excitation

Paweł Borowicz[1,2,3] and Bernhard Nickel[2]

[1] *Spectroscopy and Photochemical Kinetics Department, Max Planck Institute for Biophysical Chemistry, Am Fassberg 11, 37077 Göttingen, Germany*
[2] *Department of Photochemistry and Spectroscopy, Institute of Physical Chemistry, Polish Academy of Sciences, Kasprzaka 44/52, 01-224 Warsaw, Poland*
[3] *Department of Characterisation of Nanoelectronic Structures, Institute of Electron Technology, Al. Lotników 32/46, 02-668 Warsaw, Poland*

Correspondence should be addressed to Paweł Borowicz; borowicz@ite.waw.pl

Received 24 June 2012; Accepted 23 August 2012

Academic Editor: Gianfranco Giubileo

Copyright © 2013 P. Borowicz and B. Nickel. This is an open access article distributed under the Creative Commons Attribution License, which permits unrestricted use, distribution, and reproduction in any medium, provided the original work is properly cited.

In this paper the model developed for estimation of the diffusion coefficient of the molecules in the triplet state is presented. The model is based on the intuitive modification of the Smoluchowski equation for the time-dependent rate parameter. Since the sample is irradiated with the spatially periodic pattern nonexponential effects can be expected in the areas of the constructive interference of the exciting laser beams. This nonexponential effects introduce changes in the observed kinetics of the diffusion-controlled triplet-triplet annihilation. Due to irradiation with so-called long excitation pulse these non-exponential effects are very weak, so they can be described with introducing very simple correction to the kinetic model described in the first paper of this series. The values of diffusion coefficient of anthracene are used to calculate the annihilation radius from the data for spatially homogeneous excitation.

1. Introduction

The technique of measuring the diffusion coefficient using spatially periodic excitation was first developed by Avakian and Merrifield [1], Ern et al. [2], and Ern [3]. In those papers the authors used a pattern that consists of parallel slits to create the spatially inhomogeneous distribution of the measured species, namely, triplet excitons in anthracene crystals. The technique was modified by Nickel [4], instead of the pattern with parallel slits the interference of two laser beams was used to create spatially periodic distribution of the density of the molecules in the T_1 state. In this way the drawback of original Avakian's method, the diffraction of the light on the slits was avoided. This method was applied in measurements of the diffusion coefficient of different organic molecules [5, 6].

The main aim of this work is to take into account the effect of the joined action of the first-order decay of the molecules in the triplet state and diffusion-controlled triplet-triplet annihilation (TTA) in the kinetic model that takes into account the effects caused by spatially periodic excitation. The starting points are the intuitive treatment of the spatially homogeneous excitation [7] and the Nickel's model of TTA with spatially periodic excitation [6]. The main aim of the present approach is the introducing of the joined action of TTA and first-order decay to the term describing the kinetics of the TTA for inhomogeneous excitation—in the *diffusional relaxation* term. The derived model was applied for the evaluation of the diffusion coefficient of anthracene in the T_1 state. The values obtained with the introduced model are compared with the data obtained from the Nickel's model developed in the framework of standard Smoluchowski approach.

The temperature and viscosity dependence of diffusion coefficient is another problem discussed in this paper. The hydrodynamic theory of diffusion predicts the linear dependence between the diffusion coefficient and the ratio T/η—Stokes-Einstein (SE) model [8]. At the other side the hole theory of diffusion [9] predicts that viscosity and diffusion constant vary exponentially with the temperature. In this model diffusion is described as a process that has an activation barrier. To allow the molecule to diffuse a free space (hole) must be created in the solute. The energy that is necessary for the creation of this hole is described in terms of the activation barrier. In the hole model the diffusion coefficient tends to the limited value when temperature tends to infinity, whereas in the SE model the diffusion coefficient tends to infinity with the increase of temperature. The Stokes theory of diffusion was modified by Gierer and Wirtz [8, 10]. Instead of the continuous medium they took into account the finite dimensions of the solvent and solute molecules. They introduced to the SE model a correction which is a function of the radii of solvent and solute species.

In this work we postulate the equation for the diffusion coefficient as dependent on the T/η which combines the finite limit of the diffusion constant for large values of T/η as in the hole theory of diffusion and the linear dependence of the diffusion coefficient for small T/η as predicted by SE equation.

2. Description of the Kinetic Model

2.1. Temporal Behavior of Delayed Fluorescence after Spatially Periodic Excitation. The kinetic equation derived for spatially periodic excitation within framework of standard Smoluchowski model is the start position of the discussion. In the case of strongly dominant first-order decay: $(4\pi R_A D_T \rho_0/k_T) \ll 1\%$ and for the spatial period $d \gg R_A$ the equation for the delayed fluorescence intensity can be written in the following way [6]:

$$I_{\mathrm{DF}}(t) = C_0 4\pi R_A D_T \rho_0^2 \left(1 + \frac{R_A}{\sqrt{\pi D_T t}}\right) e^{-2k_T t} \left(1 + \frac{b}{2} e^{-\delta t}\right), \tag{1}$$

where C_0 is the constant, R_A is annihilation radius, D_T is mutual diffusion coefficient, k_T is the first-order rate constant, ρ_0 is the density of the molecules in T_1 state at the time $t = 0$, and b is the normalized parameter specifying the degree of interference. Its value varies from 0—no interference to 1—complete interference. The parameter δ (*diffusional relaxation constant*) describes the diffusional relaxation resulting from inhomogeneous (here spatially periodic) distribution of the molecules in the T_1 state at $t = 0$ and is a function of the spatial period of excitation d and the absolute diffusion coefficient D_0 (in the case of TTA $D_0 = D_T/2$):

$$\delta = \left(\frac{2\pi}{d}\right)^2 D_0 = \frac{2\pi^2}{d^2} D_T. \tag{2}$$

Equation (1) can be divided into two parts:

$$I_{\mathrm{DF}}(t) = I_{\mathrm{DF}}^{\mathrm{homo}}(t)\, \gamma_{\mathrm{DF}}^{\mathrm{period}}(t). \tag{1'}$$

The first one describes the decay of the molecules in the T_1 state after spatially homogeneous excitation in standard Smoluchowski approach:

$$\begin{aligned} I_{\mathrm{DF}}^{\mathrm{homo}}(t) &= C_0 4\pi R_A D_T \rho_0^2 \left(1 + \frac{R_A}{\sqrt{\pi D_T t}}\right) e^{-2k_T t} \\ &= k_{2A}^S(t)\, \rho^2(t), \end{aligned} \tag{3}$$

where the convention of the indications ($k_{2A}^S(t)$) is the same as in the paper [11] it means $k_{2A}^S(t)$ is the time-dependent rate parameters in the Smoluchowski original model. The modification of the "homogeneous" kinetics was described previously [7] for the case of strongly dominant first-order decay and extended to nondominant first-order decay in the first paper of this series [12].

The other term introduces the changes in the kinetics caused by spatially periodic excitation, namely, describes the diffusional relaxation of the inhomogeneous initial distribution of the molecules in the triplet state:

$$\gamma_{\mathrm{DF}}^{\mathrm{period}}(t) = 1 + \frac{b}{2} e^{-\delta t}. \tag{4}$$

This relaxation modifies the kinetics of homogeneous distribution of the molecules in the triplet state. Since TTA do not contribute directly to this term the changes in time-dependent intensity of the delayed fluorescence are caused only by the average decay of the concentration of the molecules in T_1 state in the sample. The changes in the local concentration involve the changes in the efficiency of the TTA in different areas of the sample. The lack of the direct contribution of the TTA to the diffusional distribution manifest itself by the absolute not relative diffusion coefficient appearing in the term $\gamma_{\mathrm{DF}}^{\mathrm{period}}$.

The diffusional relaxation will be influenced by the first-order decay which decrease homogeneously the concentration of molecules in the triplet state. The diffusional relaxation constant depends on the gradient in the distribution of molecules in the T_1 state between areas of the highest and the lowest concentration of the reacting species. This gradient is built by spatially periodic excitation, so one of the factors influencing the parameter δ is the spatial period d. The mobility of the molecules is represented by absolute diffusion coefficient D_0. However, due to homogeneous decay of the molecules in the T_1 state via first-order decay the initially built gradient will change with the time by joined action of the redistribution and the first-order decay. We assume that the first-order decay can be treated as dominant and the diffusional relaxation is the function of the mobility of molecules. That means that homogeneous decay do not influence the redistribution process in other way as changing the gradient via homogeneous decrease of the concentration of the molecules in the T_1 state. In such a case the parameter δ introduced as diffusional relaxation constant should be corrected by time-dependent factor. Taking into account the independence of first-order decay and the redistribution of the molecules one can represent the diffusional relaxation in terms of joined action of the first-order decay and the diffusional redistribution by introducing

the time-dependent parameter $\delta'(t) = \delta \exp(-k_T t)$ instead of δ in the periodic term:

$$\gamma_{\mathrm{DF}}^{\mathrm{period}}(t) = 1 + \frac{b}{2} e^{-\delta e^{-k_T t} t}. \tag{5}$$

So intuitively the modified equation for the time-dependent intensity of delayed fluorescence should have the form in the case of dominant first-order decay:

$$I_{\mathrm{DF}}(\mathrm{t}) = C_0 4\pi R_A D_T \rho_0^2 \left(1 + \frac{R_A}{\sqrt{\pi D_T t} e^{-k_T t}}\right) e^{-2k_T t} \times \left(1 + \frac{b}{2} e^{-\delta e^{-k_T t} t}\right). \tag{6}$$

There is also one more point in the model that should be discussed. Since, as mentioned before, in different places in the sample one has different intensity of the exciting laser light it cannot be excluded that in the areas with higher exciting intensity small components of nonexponential behavior of the sample exist. Due to irradiation with so-called long excitation pulse, where the intensity is so small that by homogeneous excitation the nonexponential behavior of the kinetics can be generally avoided, we expect to have the nonexponential behavior only in the part directly related to the TTA, it means in homogeneous term of $I_{\mathrm{DF}}(t)$. The most sensitive part in $I_{\mathrm{DF}}^{\mathrm{homo}}(t)$ in the context of nonexponential behavior is $\rho^2(t)$, because in $k_{2A}(t)$ the changes of $\rho(t)$ contribute linearly to the time-dependent rate parameter. So the most simple way to test the nonexponential behavior of the spatially periodic decay is to use the following modification of the model:

(1) the time-dependent rate parameter has the form as in the case of the intuitively modified model with first-order decay to be dominant:

$$k_{2A}(t) = 4\pi R_A D_T \left(1 + \frac{R_A}{\sqrt{\pi D_T t} e^{-k_T t}}\right), \tag{7}$$

(2) the density of the molecules the T_1 state has the nonexponential form:

$$\rho(t) = \rho_0 \frac{e^{-k_T t}}{1 + (4\pi R_A D_T \rho_0 / k_T)(A)(1 - e^{-k_T t})}, \tag{8}$$

where A donate $(1 + R_A/\sqrt{\pi D_T t} e^{-k_T t})$,

(3) the periodic part of $I_{\mathrm{DF}}(t)$ is the same as in (5).

The density described in point 2 has the form as in (4) in the first paper of this series [12], but with k_{TT} as time-dependent rate parameter defined by (7).

To sum up: the time-dependent intensity of the delayed fluorescence for nonexponential decay with spatially periodic excitation should have the form:

$$I_{\mathrm{DF}}(t) = C_0 4\pi R_A D_T \rho_0^2 \left(1 + \frac{R_A}{\sqrt{\pi D_T t} e^{-k_T t}}\right) \times \left(\frac{e^{-k_T t}}{1 + (4\pi R_A D_T \rho_0 / k_T)(A)(1 - e^{-k_T t})}\right)^2 \times \left(1 + \frac{b}{2} e^{-\delta e^{-k_T t} t}\right). \tag{9}$$

In the temperature above 150 K the contribution of the short time effect to the intensity of the delayed fluorescence decreases very fast. If the spatial period of the irradiation is enough large the diffusion relaxation resulting from inhomogeneous excitation takes place mainly for so large values of the delay t_0 that the contribution of the nonstationary part can be neglected. Since it takes place generally at the temperatures, where the diffusion coefficient D_T is large the nonexponential approximation equation (9) seems to be the proper choice in this case. However due to negligible contribution of the short-time effect the equation can be simplified by neglecting the contribution of the nonstationary term. Neglecting the ratio:

$$\frac{R_A}{\sqrt{\pi D_T t} e^{-k_T t}} \simeq 0, \tag{10}$$

one obtains the simplified dependence of $I_{\mathrm{DF}}(t)$ for spatially periodic excitation in the case of nonnegligible contribution of nonexponential effect to the kinetics:

$$I_{\mathrm{DF}}(t) = C_0 4\pi R_A D_T \rho_0^2 \left(\frac{e^{-k_T t}}{1 + (4\pi R_A D_T \rho_0 / k_T)(1 - e^{-k_T t})}\right)^2 \times \left(1 + \frac{b}{2} e^{-\delta e^{-k_T t} t}\right). \tag{9'}$$

2.2. Temperature and Viscosity Dependence of Diffusion Coefficient. The basic model of the temperature and viscosity dependence of the diffusion constant, SE model, assumes that the particle moves in continuous medium. The diffusion coefficient D_0 is a linear function of the ratio temperature to viscosity T/η:

$$D_0\left(\frac{T}{\eta}\right) = \frac{k}{6\pi r} \frac{T}{\eta}, \tag{11}$$

where k is the Boltzmann constant and r is the radius of the particle. Viscosity η is a function of temperature and it decreases with the increase of T. In SE model $D_0 \to 0$ if $T \to 0$ and $D_0 \to +\infty$ if $T \to +\infty$. The lower limit of D_0 is reasonable: with $T \to 0$ the viscosity $\eta \to \infty$, so the mobility of the molecules should be very small. The other limit: $D_0 \to +\infty$ seems to be artificial. This limit suggests that at very high temperatures the process of diffusion should be

infinitively fast, it means the infinitively large mass should diffuse through finite area within the finite time period. At the other side the hole model of the diffusion postulate the diffusion coefficient to tend to finite limit D_∞ and to be exponentially dependent on the temperature:

$$D_0(T) = D_\infty e^{-W/kT}. \quad (12)$$

In this model the process of diffusion of solute molecule is described as series of jumps between equilibrium positions of the solute molecule. The equilibrium positions are separated by barriers. This equilibriums result from the finite (nonzero) dimensions of the solvent and solute molecules. The origin of the barrier is to create of the "hole" among the solvent molecules. This "hole" is the free space where the solute molecule can migrate. The energy W is the free energy of the barrier which corresponds to the process of creating a hole in the solvent. Since the energy W depends on viscosity, the diffusion coefficient also depends on η even if it is not written explicit in (12). The hole model of diffusion takes into account the corpuscular nature of the solvent.

Since measured values of diffusion coefficient show nonlinear dependence as a function of T/η and the course of the functions seems to tend to finite limit (see Section 4) it would be sensible to postulate an equation for D_0 satisfying following conditions:

(1) $D_0 \to 0$ for $T/\eta \to 0$;

(2) for small T/η the new equation should be approximated by SE model;

(3) $D_0 \to D_\infty$ for $T/\eta \to +\infty$.

We postulate the equation in the form:

$$D_0\left(\frac{T}{\eta}\right) = A\left(1 - e^{-B(T/\eta)}\right). \quad (13)$$

The model defined by (13) will be named as *combined model* because it has T/η as an argument of the function as in the SE model and has the exponential dependence of the diffusion coefficient from the independent variable and finite limit of the diffusion constant for high temperatures as in the hole model.

Since the difference $(1 - \exp(-B(T/\eta)))$ equals to 0 for $T/\eta = 0$, $D_0(T/\eta = 0) = 0$; for $T/\eta \to +\infty$ $D_0 \to A = D_\infty$ and the expansion of (13) in Taylor series around $T/\eta = 0$ gives

$$D_0\left(\frac{T}{\eta}\right) \approx AB\frac{T}{\eta} = D_\infty B\frac{T}{\eta}. \quad (14)$$

From (11) and (14) one can obtain

$$D_\infty B = \frac{k}{6\pi r}. \quad (15)$$

The finite limit of the diffusion coefficient when the value of the argument of function tending to infinity is the great advantage of the combined one. This kind of the dependence of the diffusion coefficient shows that the mass transport tends to saturation at very high temperatures. This kind of behavior, namely, the saturation of the efficiency of the process for conditions tending to the limit is observed in the case of other transport processes. The example of the setup where the saturation is observed is charge transport in structures like Junction Field-Effect Transistors (JFET) or Metal Semiconductor Field-Effect Transistors (MESFET) [13]. The saturation effect in the electronic structures is observed for drain current for JEFT and MESFET structures [13] and as well for accumulation-mode (AM) *p*-channel silicon-on-insulator (SOI) metal-oxide-semiconductor-fiels-effect-transistor (MOSFET) or enhancement-mode (EM) *n*-channel SOI MOSFET [14]. The saturation effect in the case of electronic devices is so important that the models of charge transport developed for structures like SOI *p*-type MOSFET [15] or high electron mobility transistors (HEMTs) based on AlGaN/GaN [16] structures have this effect as an necessary condition of correctness of the model. The sublinear behavior of charge transfer with the tendency to saturation is also observed for organic crystals that is for perylene or deuterated naphtalene [17].

3. Experimental

3.1. Materials. The purification of the materials: anthracene and cis- and transisomers of 2-methylcyclohexane (DMCH), as well the preparation of the sample was described in previous articles [7, 11, 18].

3.2. Apparatus. The apparatus was described in details also in previous papers [7, 11, 18] where so-called side excitation was used. Here we will concentrate on the parts of the setup that make possible to realize two way of excitation: the side one and the bottom one. In this paper we will use the names: illumination/excitation from the side (side excitation) or from the bottom (bottom excitation). Special attention will be focused on the elements necessary to excite the sample in spatially periodic way.

In order to create the spatially periodic distribution of the molecules in the T_1 state in the sample in wide range of viscosity two options of the excitation were used. The details of the part of the apparatus generating spatially inhomogeneous distribution of the molecules in the T_1 state are presented in Figure 1. Starting from side illumination: The laser beam prepared by the fast chopper [7, 11] was reflected in the vertical direction towards mirror M8 (see scheme of the setup in [7, 11, 12]). M8 was used to reflect the laser beam horizontally to generate the homogeneous or spatially periodic distribution of the molecules in the T_1 state. One of the wall of the sample cell was partly covered with the dielectric mirror reflecting back the laser beam from Ar^+ laser. Since the coherence length of the laser beam was 50 mm and the pathway in the cuvette was equal to 10 mm the reflection of the 30 μs long pulse generated the standing wave in the sample. In the case of homogeneous excitation the cell was moved down and the excitation beam was passing the sample over the top edge of the dielectric mirror [7, 11, 18]. This option of spatially periodic excitation is presented in Figure 1(a). The

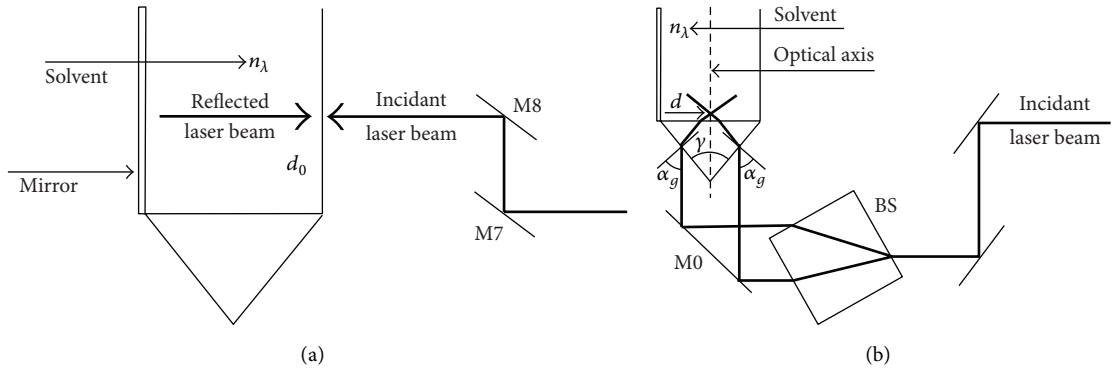

FIGURE 1: Two methods of creation of spatially periodic pattern of the exciting light: (a) excitation from the side: illumination with standing wave, (b) excitation from the bottom: illumination with two crossing beams. n_λ is the refractive index of the *cis-*/*trans*-DMCH at the wavelength equal to λ, d_0: the spatial period in the case of side excitation, d: spatial period for excitation from the bottom, γ—the angle of the prism, and α_g is the incident angle of the laser beam in the case of the bottom excitation.

other possibility of inhomogeneous excitation: the illumination from bottom is presented in Figure 1(b). The mirror signed as M7 in [7, 11] was replaced by M7′. Mirror M7′ is adjusted in such a way that it directs the laser beam to the mirror M8′ and then to the beamsplitter BS instead of reflecting it in the vertical direction to the M8. Then the laser beam was divided by beam splitter BS. Both beams were reflected by mirror M0 and entered the cell through the prism placed on the bottom wall of the cuvette. The prism angle was equal to 60°. Due to refraction of both beams on the prism walls the directions of both laser beams changed in such a way that the beams crossed in the sample and generate the spatially periodic distribution of the exciting light. In order to measure the decay in the case of homogeneous excitation from the bottom one of the crossing beam was cut-off. In the case of interference of two laser beams having equal intensities the light intensity in the maximum should be four times larger than the intensity of each interfering beam. To have the same intensity of the exciting light for homogeneous excitation and in places of positive interference of laser beams different energy of laser pulses were used for homogeneous and spatially periodic excitation. The energy of the pulse in the case of homogeneous excitation was 4 times larger in comparison with the energy of the laser pulses used for spatially periodic excitation.

The spatial period of the distribution of the exciting light can be calculated from the following equation [4]:

$$d = \frac{\lambda}{2n_\lambda \sin(\varphi)}, \tag{16}$$

where λ is the wavelength of the exciting laser light, n_λ the refraction coefficient of the solvent for the wavelength λ, and (2φ) is the angle between two crossing beams in the solvent. The angle $\varphi = \pi/2$ corresponds to the standing wave (the side illumination). The idea of spatially periodic excitation is presented in Figure 2.

3.3. Evaluation Procedure. The data were fitted using the following procedure. First the decies obtained for spatially homogeneous excitation were fitted with intuitively modified model [7]:

$$I_{\mathrm{DF}}(t) = P_0 + P_1\left(1 + \frac{P_2}{e^{-t/P_3}\sqrt{t}}\right)e^{-2t/P_3}, \tag{17}$$

where P_0 is a dark current, P_1 is the amplitude, P_2 will be called Smoluchowski parameter ($P_2 = R_A/(\pi D_T)^{1/2}$, and P_3 is the first-order decay time ($P_3 = {k_T}^{-1}$). Obtained from the fits of homogeneously excited decies the parameters P_2 and P_3 were used in the fitting of decies measured for spatially periodic excited samples. To fit the periodically excited decies the following functions were used:

$$I_{\mathrm{DF}}(t) = P_0 + P_1\left(1 + \frac{P_2}{\sqrt{t}}\right)\left(1 + P_4 e^{-t/P_5}\right)e^{-2t/P_3}, \tag{18}$$

$$I_{\mathrm{DF}}(t) = P_0 + P_1\left(1 + \frac{P_2}{e^{-t/P_3}\sqrt{t}}\right)\left(1 + P_4 e^{-(te^{-t/P_3})/P_5}\right)e^{-2t/P_3}, \tag{19}$$

$$I_{\mathrm{DF}}(t) = P_0 + P_1\left(1 + \frac{P_2}{e^{-t/P_3}\sqrt{t}}\right)\left(1 + P_4 e^{-(te^{-t/P_3})/P_5}\right) \times \left(\frac{e^{-t/P_3}}{1 + P_6\left(1 + \left(P_2/e^{-t/P_3}\sqrt{(t)}\right)\right)\left(1 - e^{-t/P_3}\right)}\right)^2, \tag{20}$$

where P_4 describes the degree of the interference, P_5 is the diffusion relaxation time ($P_5 = \delta^{-1}$), and P_6 plays the role of the indicator of nonexponential behavior and equals

$$P_6 = \frac{4\pi R_A D_T \rho_0}{k_T}. \tag{21}$$

The function defined by (18) describes the model developed by Nickel [4–6] within standard Smoluchowski approach. It was used here as a reference. The function defined by (19) can be treated as intuitively modified (18) and describes the condition of strongly dominant first-order decay. The equation

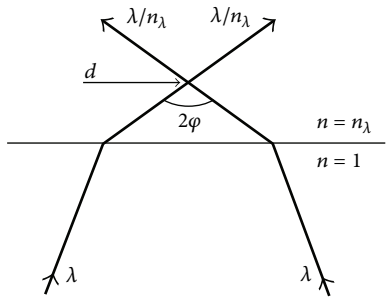

Figure 2: The idea of the creation of the spatially periodic excitation in the sample. Two laser beams having the wavelength equal to λ in air cross each other in the sample and create the spatial pattern of the light with period equal to d. The angle between crossing beams equal 2φ, the refractive index of the sample equals to n_λ.

(20) introduces to (19) the nonexponential approximation on the lowest possible level (see Section 2).

The functions given by (19) and (20) take into account both components of the decay in intuitively modified model: the short time part and the stationary part. The diffusional relaxation has to play important role in the kinetics on different time scale in comparison with short time effect. Otherwise it will be impossible to differentiate between these two components of the model in the case of analysis of the data measured with spatially periodic excitation of the sample.

The measurements of the diffusion coefficient were performed in the temperature range from 135 K to 155 K. The viscosity of the mixture solvent changes over four orders of magnitude. In the vicinity of the ends of the temperature range the differences in time scales of the short time effect and diffusional relaxation may be so large that the simplified equation for the $I_{\mathrm{DF}}(t)$ may offer more stable fit than (19) or (20). Taking the diffusion coefficients used in previous papers [7, 11] and the approximate value of annihilation radius equal to 1 nm and the spatial period of excitation as used in the experiment one can estimate the contributions of the short time term and the diffusional relaxation term to the whole decay of the delayed fluorescence. The measurements were done for two values of spatial radius: 119 nm and 305 nm. In the next paragraph the estimation of the short time term and the diffusional relaxation term will be presented.

In the case of low viscosity where the diffusion is fast the short time effect decay also very fast. In order to have reasonable time for the diffusional relaxation one should excite the sample with enough large spatial period. For example, in the case of the decay measured at $T = 150$ K after the delay equal to about 2 ms the term describing short time effect equals to about 0.06 whereas the diffusional relaxation term: $\exp(-\delta t \exp(-k_T t))$ equals to ~0.60 if the spatial period of excitation equals to about 305 nm. After the delay equal to 20 ms the short time term equals to 0.02 and the diffusional relaxation equals to about 0.28. So, if the spatial period of excitation is enough large the diffusional relaxation mainly takes place in the delay range where flow can be approximated with stationary part of the intuitively modified Smoluchowski equation. Since the bottom excitation gives small signal, because only small part of the illuminated part of sample contributes to the measured signal the number of the fitted parameter should be limited in order to make the fitting procedure as stable as possible. In such a case (20) should be simplified:

$$I_{\mathrm{DF}}(t) = P_0 + P_1\left(1 + P_4 e^{-(te^{-t/P_2})/P_5}\right) \times \left(\frac{e^{-t/P_3}}{1 + P_6\left(1 - e^{-t/P_3}\right)}\right)^2. \quad (20')$$

At the other side in high viscosities the diffusional relaxation can also be important for longer delay than the short time effect. For example, in the case of the decay measured at 135 K and after the delay equal to about 3 ms the short time term decreases to the value equal about 0.09 whereas the diffusional relaxation term equals to about 0.95 if the spatial period of excitation equals to 119 nm. After 20 ms the short time term decreases to 0.06 and diffusional relaxation term to about 0.80. So, as in the case of high temperature the main part of diffusional relaxation takes place when the process can be described with stationary part of the intuitively modified Smoluchowski equation. Here the intensity of the delayed fluorescence is low due to low mobility of the molecules. In such conditions the fit of the function with minimum number of important parameters can give more stable results than the fit of the whole function defined by (19). The simplified equation (19) has the following form:

$$I_{\mathrm{DF}}(t) = P_0 + P_1\left(1 + P_4 e^{-(te^{-t/P_2})/P_5}\right) e^{-2t/P_3}. \quad (19')$$

The other approximation used here is the same as in previous papers [7, 11]: it means that modified initial condition introduced by Nickel et al. [19] have significant influence on the initial part of the decay. In those papers the decay was divided into *anti-Smoluchowski* and *Smoluchowski* time ranges. Within the *anti-Smoluchowski* time range the modified initial conditions introduce to the temporal behavior of the decay significant changes in comparison with standard Smoluchowski behavior. In the *Smoluchowski* time range the course of the decay of the delayed fluorescence is the same for both types of initial conditions. The points are systematically cut off from the beginning of the decay of spatially homogeneous excited samples. In this way the part of the decay where the modified initial condition introduce the important changes to the kinetics is removed. The parameters P_2 and P_3 were obtained from the evaluation of the decies measured for the spatially homogeneous excited samples. They are kept constant in the case of the fitting of the spatially periodic excited samples. The values of the parameters P_4, P_5 and in the case of nonexponential behavior P_6 are obtained from *Smoluchowski* time range of spatially periodic excited decay. The *anti-Smoluchowski* and *Smoluchowski* time ranges are assumed to be the same in the case of homogeneously and spatially periodic excited samples. The reason to avoid the *anti-Smoluchowski* time range in the fitting procedure is the same as in previous papers:

(i) the modified initial conditions do not affect the general idea of the joined action of two processes: the first-order decay and TTA;

(ii) the mathematical description of the kinetics is much simpler for the standard Smoluchowski initial conditions.

The *Smoluchowski*, *anti-Smoluchowski* time range are presented in Figure 3 together with the delay range of particular interest.

The values of the parameters P_4, P_5, and eventually P_6 were obtained as follows. The functions defined by (18) ÷ (20) were fitted to the measured decies with the systematic cutting off the points from the beginning. Using this procedure one obtains the parameters as functions of the delay, t_0. In the case of (19) for exponential behavior or (20) in the case of nonexponential behavior one should obtain the constant values (within the accuracy of the measurement and the fitting procedure) of parameters P_4, P_5, and eventually P_6 in the time range of particular interest (see Figure 3). In the case of the decies measured near the limits of the temperature range the simplified functions: equation $(19')$ for exponential behavior and $(20')$ for nonexponential case were fitted and the results were compared with the fits performed for the whole functions (see (19) and (20)). The option giving more stable fit and precise results were taken to the further analysis. The values of parameters P_4 and P_5 obtained from the fitting of (18) were taken as reference. The values of the parameters were averaged over the range of particular interest. The mutual diffusion coefficient was calculated from the parameter P_5:

$$P_5 = \delta^{-1} = \frac{d^2}{2\pi^2 D_T} \Longrightarrow 2D_0 = D_T = \frac{d^2}{2\pi^2 P_5}, \tag{22}$$

where the spatial period d was calculated for the wavelength of the Ar^+ laser $\lambda = 363.3$ nm and the refractive index of *cis*/*trans*-DMCH. The refractive index n_λ of the mixture solvent was measure and published previously [20].

The temperature and viscosity dependence of the diffusion coefficient was examined with the following procedure. First the linear functions was fitted to the values of the absolute diffusion coefficient calculated from (22):

$$\frac{D_T}{2} = D_0 = a_0 \frac{T}{\eta}, \tag{23a}$$

$$\frac{D_T}{2} = D_0 = a_1 \frac{T}{\eta} + b_1. \tag{23b}$$

Since in the SE model $D_0((T/\eta) = 0) = 0$ the coefficients a_0 and a_1 obtained from fits of (23a) and (23b) should be equal within experimental error. The coefficient b_1 can be treated as an additional component of the standard deviation of D_0. The contribution of this component should be important in high viscosities. Also the other model of temperature/viscosity dependence of the diffusion constant was fitted to the experimental points:

$$\frac{D_T}{2} = D_0 = a_3 \left(1 - e^{-b_3(T/\eta)}\right). \tag{24}$$

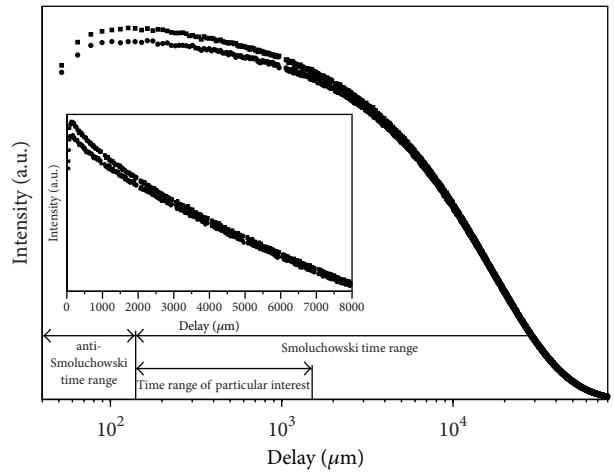

Figure 3: The influence of the modified initial conditions and the spatially periodic excitation. The main picture: the intensity of the delayed fluorescence of anthracene measured at 143 K. The upper curve presents spatially periodic excitation, lower—homogeneous. The ordinate is presented in logarithmic scale in order to expand the initial period where the differences between the temporal behavior of the homogeneously and spatially periodic excited sample are significant. The *anti-Smoluchowski* time range the extent of the delay where modified (Nickel's) initial conditions introduce significant changes to the kinetics of diffusion controlled TTA, the *Smoluchowski* time range the extent of the delay where the temporal behavior of the sample is the same for both type of initial conditions. The time range of particular interest the extent of the *Smoluchowski* time range where the temporal behavior of homogeneously and spatially periodic excited sample are significantly different. Insert: the initial part of the main picture with the ordinate in linear scale.

The values of diffusion coefficient were calculated from both models: SE model (see (23a), (23b), and combined model (24)).

The annihilation radius R_A was calculated from P_2 (Smoluchowski) parameter obtained from the fits of the decies of homogeneously excited sample:

$$R_A = P_2 \sqrt{\pi D_T}, \tag{25}$$

using values of D_T calculated from the both models of temperature/viscosity dependence of the diffusion coefficient. The values of R_A calculated for the experimental data resulting from measurements for short and middle excitation pulses are compared with those obtained for the long excitation pulse [7, 11]. Also the values of the annihilation radius calculated with the diffusion coefficient obtained from SE and combined models are compared with each other.

4. Results and Discussion

4.1. Comparison of the Nickel's and Modified Approaches, Exponential Decay. In Figure 4 there is presented the comparison of the fit of two models: original Nickel's approach (18) and intuitively modified one (19). Since the parameters

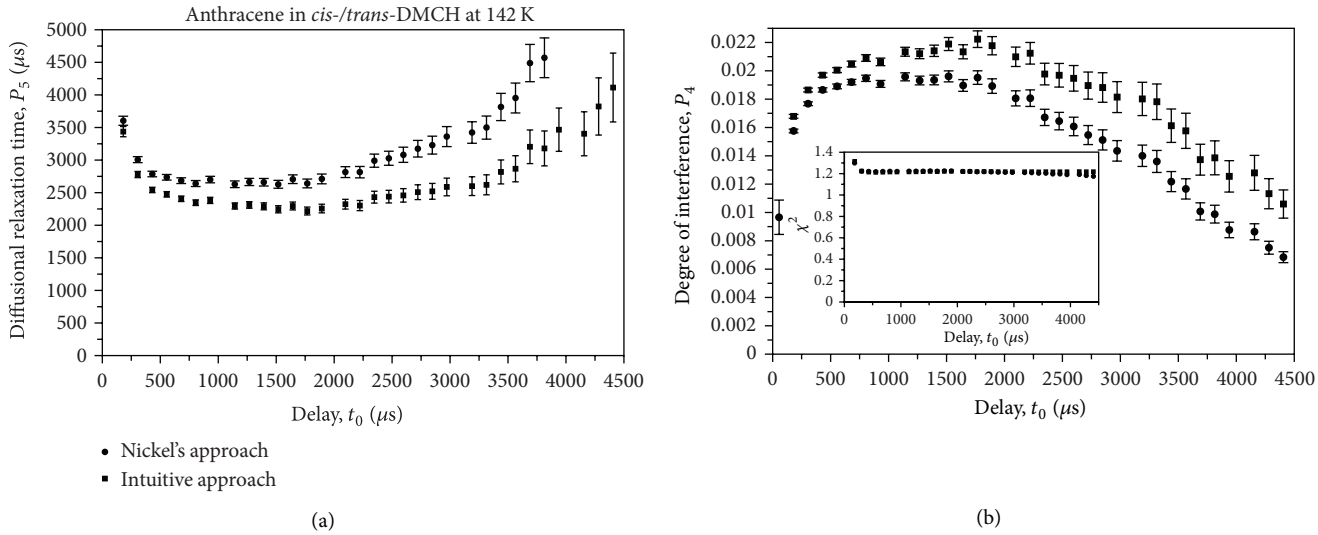

FIGURE 4: The diffusional relaxation time (part (a)) and the degree of interference (part (b)) as dependent on the delay. The comparison of two models: circles: Nickel's approach, squares: intuitively modified model. Both models are applied in the form of dominant first-order decay. The insert presents χ^2 function as dependent on t_0.

P_2 and P_3 were taken from the fit of homogeneously excited decay they are not presented here. The comparison is reduced to the diffusional relaxation time P_5, —Figure 4(a) and the degree of interference P_4—Figure 4(b). Both parameters were obtained from the fitting procedure performed for the decay measured at 142 K. The parameters P_4 and P_5 are presented as dependent on the delay, t_0. The course of the parameters are similar for both models. In the case of P_5 (Figure 4(a)) after the decrease for $t_0 <$ ~500 μs the values reach shallow minimum which can be treated constant within the accuracy of the measurement and fitting procedure. For $t_0 >$ ~2500 μs the diffusional relaxation time has clear tendency to grow up with the increase of the delay. The values of P_5 obtained from the intuitive model are about 500 μs smaller than those from Nickel's original approach in the range of t_0, where the plateau is reached. The course of the parameter P_4 (Figure 4(b)) as a function of the delay corresponds to the course of P_5. For $t_0 <$ 500 μs the values of the degree of interference increase with the increase of the delay. In the range 500 μs $< t_0 <$ 2500 μs there is a shallow maximum where the values can be treated as constant. For $t_0 >$ 2500 μs the values of P_4 decrease with the increase of the delay. The insert in Figure 4(b) presents χ^2 as a function of t_0. For the delay larger than 500 μs the values of the χ^2 can be treated as constant and equal to about 1.2 for both models.

In Figure 5 there are presented the values of diffusion coefficient D_T (average values) calculated from original Nickel's and intuitively modified model as a function of T/η in the range below 0.12 K/m Pa s (what corresponds to the temperature below 149 K). The experimental data are presented together with the fit of SE model. The measurements performed in the range $T/\eta <$ 0.055 K/m Pa s (the temperature below 145 K) were done for the side excitation. In the case of higher temperatures the larger spatial period of excitation was necessary. These measurements were done

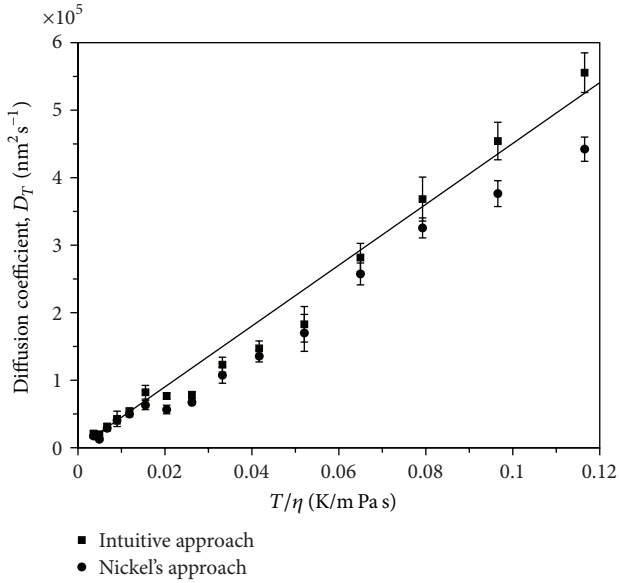

FIGURE 5: The mutual diffusion coefficient D_T as dependent on the ratio T/η for abscissa below 0.12. The experimental points are compared with fitted SE model. The values of D_T calculated from Nickel's approach have the tendency to deviate from the SE model for $T/\eta >$ ~0.018. The results from intuitively modified model show better agreement with SE model. Within the range ~0.018 $< T/\eta <$ ~0.07 the experimental results from modified model still show the difference from SE model.

for bottom excitation. From the course of the experimental values can be deduced that original Nickel's approach gives the values of the diffusion coefficient that have a tendency to deviate from the linear SE model. This tendency can be corrected introducing the intuitive modification to the

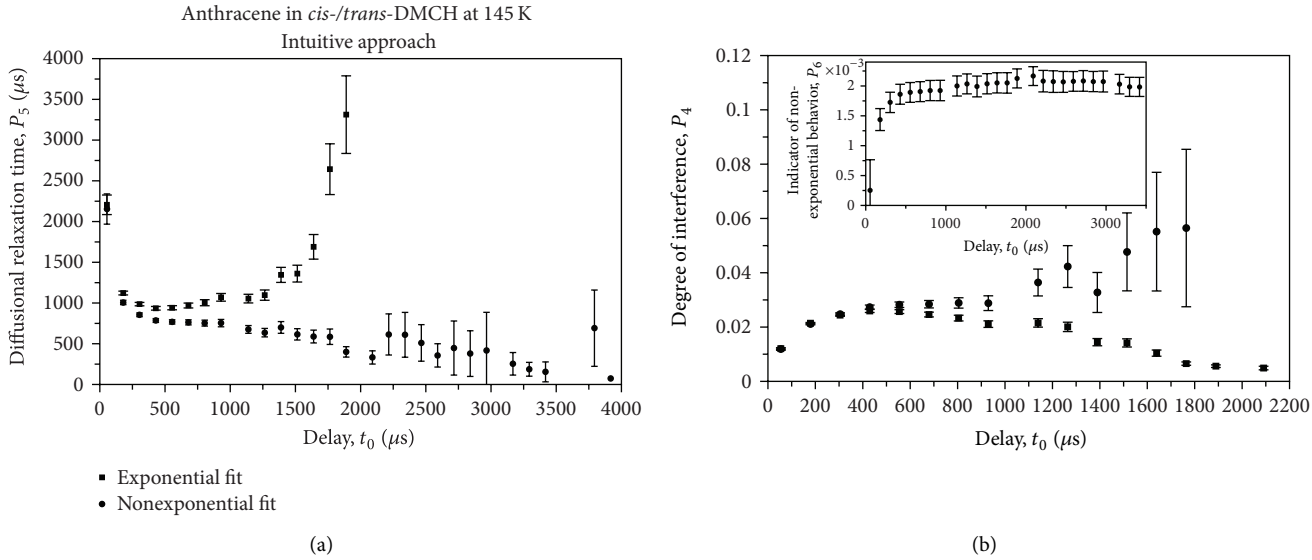

FIGURE 6: The diffusional relaxation time (part (a)) and the degree of interference (part (b)) as dependent on the delay, t_0, measured at 145 K. The comparison of two versions of the modified model for spatially periodic excitation: squares—exponential fit, circles—nonexponential fit. The insert presents the indicator of nonexponential behavior as a function of the delay.

Nickel's formula for the temporal dependence of the intensity of delayed fluorescence. The correction gives the results consistent with SE model in the range 0.055 K/m Pa s < T/η < 0.12 K/m Pa s. The difference between experimental diffusion coefficient and SE model in the range ~0.015 K/m Pa s < T/η < ~0.055 K/m Pa s is not fully corrected with the intuitive modification of the Nickel's equation. The additional difference between the experimental values and SE model results from nonexponential decay of the spatially periodic excited sample. This is due to the side excitation of the sample within this range of T/η where the energy of the exciting pulse was significantly larger than in the case of bottom excitation (see Section 3).

4.2. Nonexponential Contribution to the Modified Model in the Case of Spatially Periodic Excitation. The parameters P_5 and P_4 as a function of the delay are presented in Figure 6, where the values obtained from exponential and nonexponential models (see *Description of the model*, part *Temporal behavior of delayed fluorescence after spatially periodic excitation*) are compared. In Figure 6(a) there is presented diffusional relaxation time P_5 as a function of the delay. For exponential model the values of P_5 decrease with the increase of the delay for t_0 < ~400 μs. For ~400 μs < t_0 < ~1300 μs the values obtained from exponential model show shallow minimum. The values within this range of t_0 can be treated as constant within experimental error. For t_0 > ~1300 μs the rapid increase of P_5 with the delay is observed. In the case of nonexponential the course of P_5 is similar to the exponential case: for t_0 < ~400 μs the decrease of P_5 with the increase of the delay is observed. For ~400 μs < t_0 < ~1400 μs the values of P_5 can be treated as scattered around the constant. For t_0 > ~1400 μs the parameter P_5 has tendency to decrease with the increase of t_0. Also the increase of the standard deviation ΔP_5 is observed for t_0 > ~2200 μs. The behavior of degree of interference—Figure 6(b) corresponds to that of diffusional relaxation time. For t_0 < ~400 μs the values of P_4 obtained from both types of modified model (exponential and nonexponential) increase with the increase of the delay. In the case of exponential fit parameter P_4 reaches the shallow maximum for ~400 μs < t_0 < ~600 μs and for larger t_0 the decrease of the value of P_4 with the increase of the delay is observed. The values of P_4 resulting from nonexponential fit can be treated as constant within the accuracy of the measurement and fitting procedure for ~400 μs < t_0 < ~1000 μs. For t_0 > ~1000 μs the values of the parameter P_4 are scattered and the standard deviation ΔP_4 is much larger than for the delay below 1 ms. The insert in Figure 6(b) presents the indicator of nonexponential behavior—P_6. Although the values are very small (not larger than 0.003) they can be treated as constant within the presented accuracy for the delay between ~400 μs and a few milliseconds.

In Figure 7 there is presented diffusion coefficient obtained from kinetic model with taking into account the nonexponential character of the decay in the range ~0.015 K/m Pa s < T/η < ~0.055 K/m Pa s. The presented values were calculated from exponential: T/η < ~0.015 K/m Pa s and nonexponential: ~0.015 K/m Pa s < T/η < ~0.055 K/m Pa s fits. The "experimental" values of the diffusion constant are presented together with the SE model. The range of T/η from 0.003 to 0.052 K/m Pa s corresponds to the temperature range 135 K ÷ 145 K. The difference between SE model and the result of the fitting of exponential modified model of the periodically excited delayed fluorescence increases with the increase of T/η. The nonexponential model of the decay seems to reproduce better the SE dependence of the diffusion coefficient than the exponential approximation of the decay. The effect is small but the tendency seems to be unequivocal.

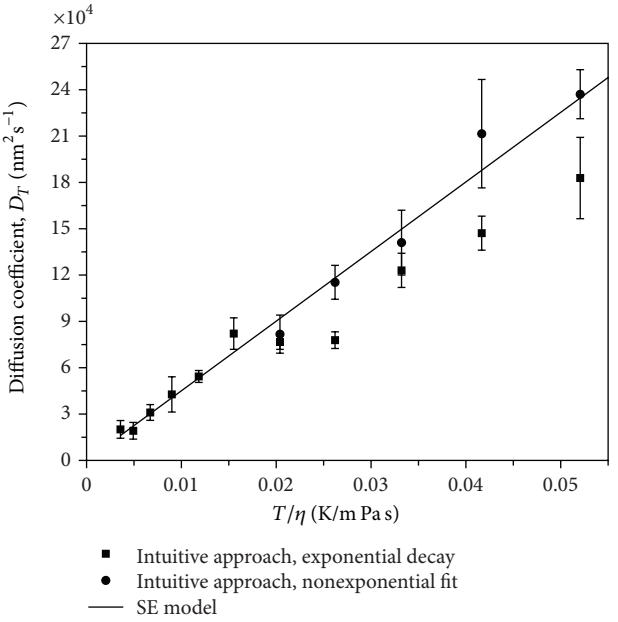

Figure 7: The mutual diffusion coefficient as a function of T/η in the range below 0.052. The comparison of the values calculated from fits of the exponential (squares) and nonexponential (circles) intuitively modified model of the temporal behavior of delayed fluorescence. The straight line represents the SE model. The values calculated from exponential model of $I_{DF}(t)$ show the deviation from SE model in the range from 0.02 to 0.052 K/(m Pa s). The values calculated from nonexponential model show better agreement with the SE model in this range of T/η.

4.3. Negligible Short Time Effect. As mentioned in Evaluation procedure in some cases the short time effect can be neglected and the simplified functions of $I_{DF}(t)$ can be used. In Figure 8 there is presented an example of evaluation of the decay measured at 155 K. Here the results of the fitting procedure obtained from whole and simplified kinetic models are compared. The course of the parameters obtained with or without the contribution of the short term are almost the same. The diffusional relaxation time (Figure 8(a)) shows the increase of the value of the parameter P_5 for $t_0 < \sim 250\,\mu$s. For the delay from the range $\sim 250\,\mu$s to ~1 ms the values are scattered around the constant. For $t_0 > 1$ ms the increase of the standard deviation ΔP_5 and the value of P_5 is observed. The increase of ΔP_5 reflects the decrease of the contribution of the diffusional relaxation to the total decay. The values obtained for the P_4 parameter (Figure 8(b)) show the decrease as a function of the delay in the range: $t_0 < \sim 250\,\mu$s. For $\sim 250\,\mu\text{s} < t_0 < \sim 700\,\mu$s the values of P_4 can be treated as scattered around the constant. The dispersion of the values obtained with the neglecting of the short time effect $(20')$ is significantly smaller in comparison with the data resulting from the fit of (20). For $t_0 > \sim 700\,\mu$s the the values of P_4 decrease with the increase of the delay. The parameter P_4 tends asymptotically to zero. The values of χ^2 are presented in the insert in Figure 8(b). The values of χ^2 are constant and equal to about 1.05 for both version of the kinetic model.

In Figure 9 there is presented similar comparison as in Figure 8. Here however, the evaluation was performed for the decay measured at 136 K. The complete function of the kinetic model was defined by (19), the simplified one by $(19')$. In Figure 9(a) the diffusional relaxation time is presented as dependent on the delay. In the case of the fit with short time term included only first two points are presented in the plot. The other values obtained from the fit of (19) are much larger than the scale and their standard deviation is larger than the value of the parameter. So they are omitted in the plot. The results of the fit of $(19')$ show the decrease of P_5 with the increase of the delay for $t_0 < \sim 800\,\mu$s. For $\sim 800\,\mu\text{s} < t_0 < \sim 8000\,\mu$s the values of the diffusional relaxation time can be treated as scattered around the constant. The standard deviation ΔP_5 grow up with the delay. This behavior reflects the decrease of the contribution of the diffusional relaxation to the whole decay with the increase of the delay. For $t_0 > \sim 8$ ms the decrease of the P_5 with the increase of the delay is observed. The degree of interference shows similar behavior—Figure 9(b). The data obtained from fit of (19) (with short-time term included) are not presented due to the standard deviation overcoming 100% of the value of the parameter. In the case of the analysis neglecting short time effect the values of P_4 are scattered around the constant for $t_0 < 8$ ms. The exception is the first point which standard deviations is larger than the value. The increase of the standard deviation ΔP_4 is observed as in the case of the diffusional relaxation time. This increase is very clear for the delay above ~5.5 ms. For $t_0 > \sim 8$ ms the increase of the P_4 with the increase of the delay is observed. Also the increase of ΔP_4 for the delay above 8 ms is much more significant. From the course of P_4 and the ratio $\Delta P_4/P_4$ one can deduce that the contribution of the diffusional relaxation to the whole decay decreases significantly within the delay range $\sim 5.5\text{ ms} < t_0 < 8$ ms. For the delay larger than 8 ms this contribution seems to be negligible. The insert in the Figure 9(b) presents the χ^2 as dependent on the delay. The value obtained for the fit of (19) are spread between 1 and 2.4, whereas the values of χ^2 resulting from fit of $(19')$ are constant and equal to 1 for $t_0 > \sim 500\,\mu$s.

It seems that in the case of periodically excited samples in some cases the simplified functions with reduced number of parameters give better results than the complete one. This is due to the complicated temporal dependence of the delayed fluoresce which is described with function having up to 7 parameters. In some cases simplification of fitted function results in avoiding the parameters that values are negligible. This gives in turn more stable fit and more reasonable results.

4.4. Viscosity and Temperature Dependence of the Diffusion Coefficient. In Figure 10 there is presented the diffusion coefficient D_T as dependent on T/η. Together with experimental points fitted models are presented: SE model and a combined model. The course of experimental points shows that the both models give the similar values of the diffusion coefficient up to $T/\eta = \sim 0.15$ K/m Pa s. For larger values of T/η the diffusion coefficient shows the deviation from SE model towards lower values. The other model seems to

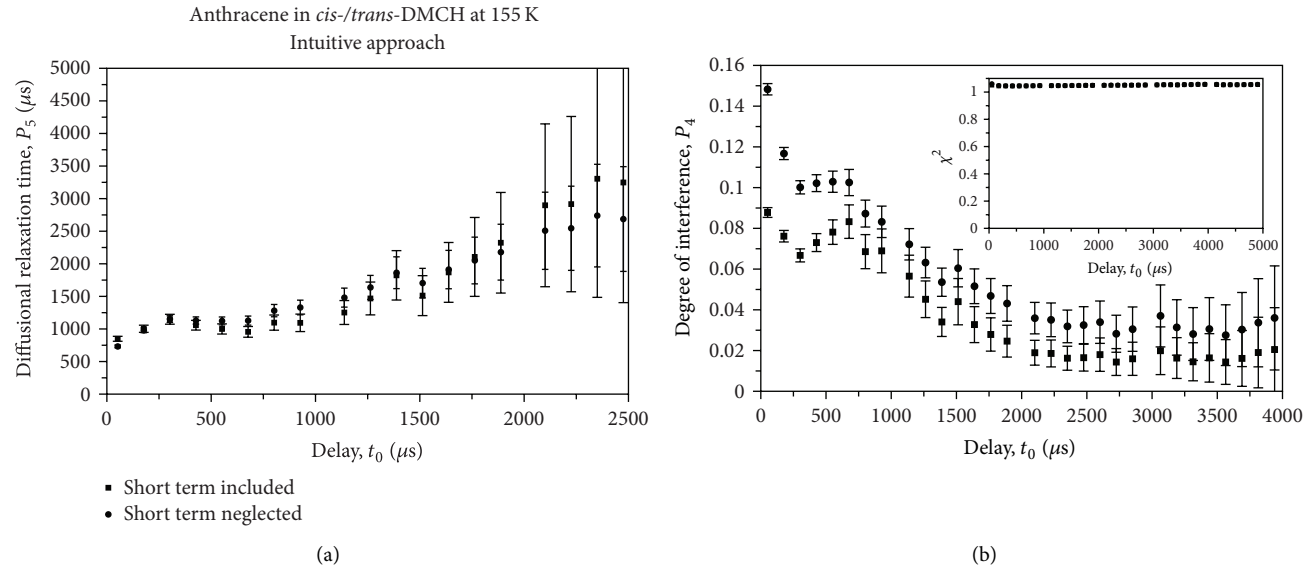

Figure 8: Diffusional relaxation time (a) and the degree of interference (b) as dependent on the delay. The comparison of the exponential model of temporal behavior of the intensity of delayed fluorescence in the case of included short time effect (squares) and neglected short time effect (circles). Fits were done for the decay measured at 155 K with bottom excitation. Both variations of the model show almost the same course of the presented parameters. The insert presents the χ^2 as dependent on t_0. The values of are equal to about 1.05.

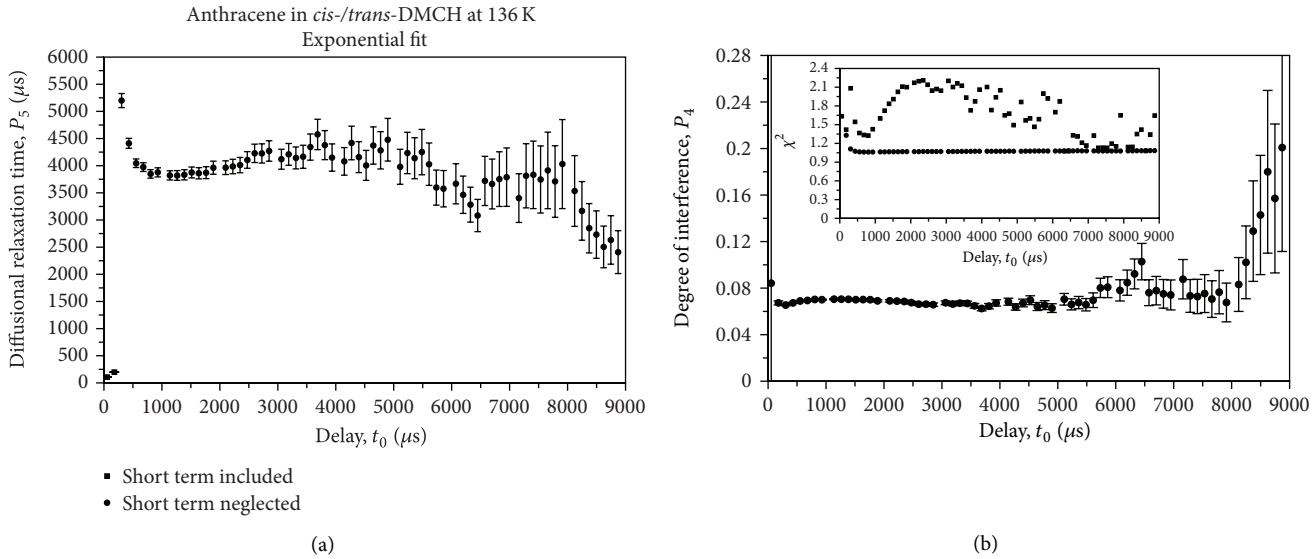

Figure 9: The same comparison as presented in Figure 8 in the case of measurement at 136 K. The values of diffusional relaxation time and degree of interference obtained for included short time term are omitted, because they are pathologically large and their standard deviations overcome 100% of the values. The function χ^2 (insert in the part (b)) shows the quality of both fits. In the case of neglected short time term the values of χ^2 equal to about 1.05 for $t_0 > \sim 500\ \mu$s, whereas for the other case the values of χ^2 are spread between 1 and 2.5.

reproduce better than the SE model the course of the experimental points. The values of D_T extrapolated to the room temperature with different models are as follows,

(1) SE model: $(1.50 \pm 0.02) \times 10^9\ \text{nm}^2\ \text{s}^{-1} = (1.50 \pm 0.02) \times 10^{-1}\ \text{cm}^2\ \text{s}^{-1}$,

(2) combined model: $(1.43 \pm 0.16) \times 10^6\ \text{nm}^2\ \text{s}^{-1} = (1.43 \pm 0.16) \times 10^{-4}\ \text{cm}^2\ \text{s}^{-1}$.

Let us compare the diffusion coefficient measured for organic molecules (having the size similar to anthracene) in organic solvents at room temperature with the data extrapolated with both models. The collection of the anthracene absolute diffusion coefficients (D_0) in different solvents can be found in [6]. The values at 25°C are in hexane $(3.15 \div 3.18) \times 10^{-5}\ \text{cm}^2\ \text{s}^{-1}$, in octane $1.97 \div 2.04 \times 10^{-5}\ \text{cm}^2\ \text{s}^{-1}$, in hexadecane $0.536 \div 0.545 \times 10^{-5}\ \text{cm}^2\ \text{s}^{-1}$, in perfluororohexane $(1.80 \pm 0.03) \times 10^{-5}\ \text{cm}^2\ \text{s}^{-1}$, and in

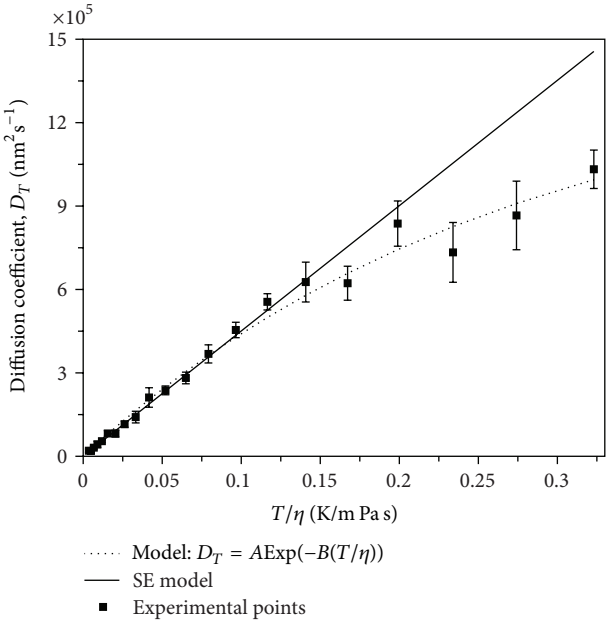

Figure 10: The comparison of experimental data (squares) of the mutual diffusion coefficient D_T as dependent on temperature and/or viscosity. Presented data are calculated with application of two models: SE model (straight line) and combined model (dotted line).

methylcyclo-hexane $(1.61 \pm 0.03) \times 10^{-5}\,\text{cm}^2\,\text{s}^{-1}$. The diffusion constant of pyrene and 9,10-diphenylanthracene in hexane equal to $(2.93 \pm 0.04) \times 10^{-5}\,\text{cm}^2\,\text{s}^{-1}$ and $(1.80 \pm 0.02) \times 10^{-5}\,\text{cm}^2\,\text{s}^{-1}$, respectively. Taking into account that $D_T = 2D_0$ the cited data can be summed up: the absolute diffusion coefficient at room temperature in the range between 10^{-5} and $10^{-4}\,\text{cm}^2\,\text{s}^{-1}$. The value of D_0 extrapolated with the combined model $\sim 0.7 \times 10^{-4}\,\text{cm}^2\,\text{s}^{-1}$ can be treated as reasonable, whereas the values calculated with SE model overestimate the experimental day by a few orders of magnitude.

The expansion in the Taylor series of the combined model gives the product of the coefficients a_3 and b_3 (see (24)) equal to $(5.3 \pm 1.1) \times 10^6\,\text{nm}^2\,\text{K}\,(\text{m Pa s}^2)^{-1}$, where the standard deviation $\Delta(a_3 b_3)$ was calculated from

$$\Delta(a_3 b_3) = \left(\Delta a_3^2 + \Delta b_3^2\right)^{1/2}. \tag{26}$$

The slope obtained from the fit of SE model equals to $(4.51 \pm 0.05) \times 10^6\,\text{nm}^2\,\text{K}\,(\text{m Pa s}^2)^{-1}$. Taking into account standard deviations of the above discussed quantities both presented above values can be treated as equal.

4.5. Annihilation Radii. Using the diffusion coefficients D_T obtained from both discussed above models the annihilation radii were calculated. In Figure 11 there are presented annihilation radii obtained for the measurements with short excitation pulse and spatially homogeneous excitation. The data presented in Figure 11 consist of values calculated from exponential and nonexponential approaches of the temporal dependence of the delayed fluorescence intensity. In Figure 11(a) the values of annihilation radii calculated with D_T from SE model are presented. For the temperature range 132 K ÷ 146 K the values of R_A are calculated from parameter P_2 obtained from exponential fit of $I_{\text{DF}}(t)$ (squares). In the case of the temperature range 142 K ÷ 150 K the values are taken from nonexponential fit (circles). The values calculated from exponential model of the kinetics of TTA can be treated as constant for the temperature range 138 K ÷ 144 K. For the temperatures below 138 K the the values of R_A decrease with the decrease of the temperature. The increase of the standard deviation ΔR_A with the decrease of the temperature in the range 132 K ÷ 138 K reflects the growing up uncertainty of the diffusion coefficient D_T with the decrease of the temperature. For the temperatures 145 K and 146 K the R_A obtained from exponential kinetics has the tendency to grow up with the temperature. In the case of the temperature above 146 K the values of the annihilation radii were not average, because there was no range of the delay t_0 (for $t_0 < \sim 10$ ms) where P_2 parameter can be treated as constant in the case of exponential model. In the case of nonexponential fit the values of R_A were calculated for the decies measured in the temperature range 142 K ÷ 150 K. The values obtained from nonexponential fit are constant within this temperature range. For the temperature between 142 K and 144 K the values of R_A resulting from exponential and nonexponential models of the decay are equal. In Figure 11(b) there is presented annihilation radius calculated from the combined model. The values of R_A are presented as dependent on the temperature. The behavior of R_A as a function of the temperature is practically the same in the case of Figure 11(b) as described above for Figure 11(a). The only difference between Figures 11(a) and 11(b) is the behavior of standard deviation ΔR_A in the temperature range 132 K ÷ 138 K. In the case of Figure 11(b) it is constant what shows that the standard deviation of D_T does not increase with the drop of the temperature as in the case of SE model.

In Figure 12 there is presented the annihilation radius R_A as a function of temperature for the short excitation pulse and the model based on the non-Fickian treatment of TTA [11]. The partition of the temperature range between exponential and nonexponential part is the same as in Figure 11. Parts (a) and (b) present the data calculated for the same model of the viscosity and/or temperature dependence of D_T as in the case of Figure 11:

(i) part (a): D_T calculated from SE model;

(ii) part (b): D_T calculated from combined model.

In the case of Figures 12(a) and 12(b) the course of R_A as a function of the temperature is similar to that presented in Figures 11(a) and 11(b). The are two differences between the behavior presented in Figures 12(a) and 12(b), and Figures 11(a) and 11(b). First the annihilation radii calculated from the non-Fickian treatment are larger in comparison with that from the intuitive modification of Smoluchowski equation. The average value for the "intuitive" R_A equals to about 0.6 nm, whereas the non-Fickian approach gives the value of annihilation radius equal to about 1 nm. This discrepancy was already discussed in previous paper [11]. It

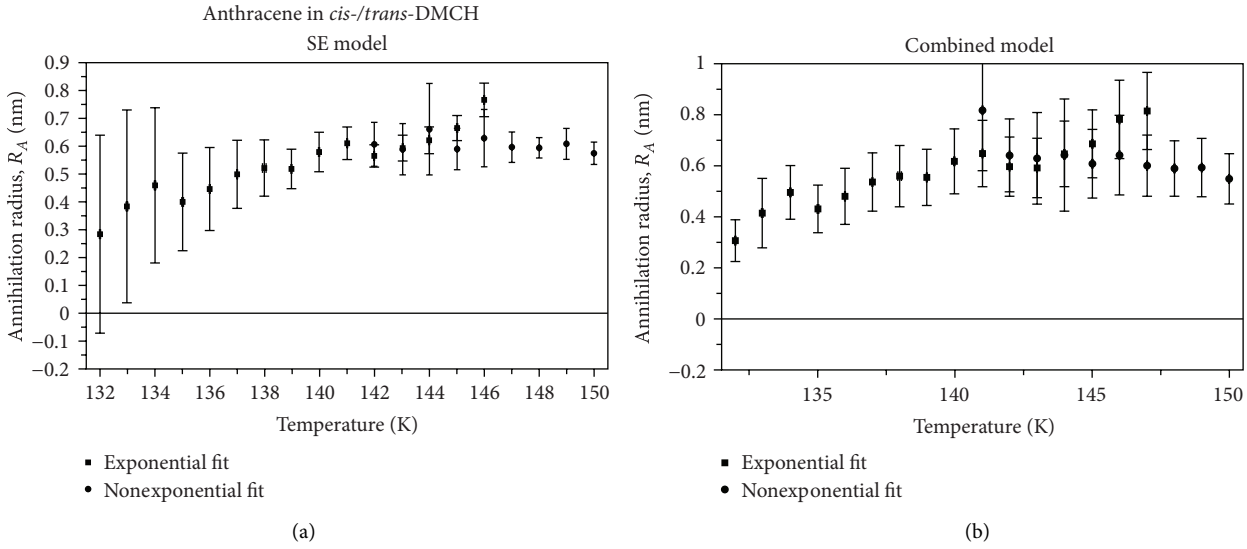

FIGURE 11: The annihilation radius calculated using the values of mutual diffusion coefficient obtained from spatially periodic excitation and different models of temperature and/or viscosity dependence of D_T: (a) SE model and (b) combined model. The P_2 parameter was calculated from the intuitively modified Smoluchowski model [7] of temporal behavior of the intensity of delayed fluorescence. The plots present the combination of exponential and nonexponential versions of the $I_{DF}(t)$. The experimental data were measured with the short excitation pulse.

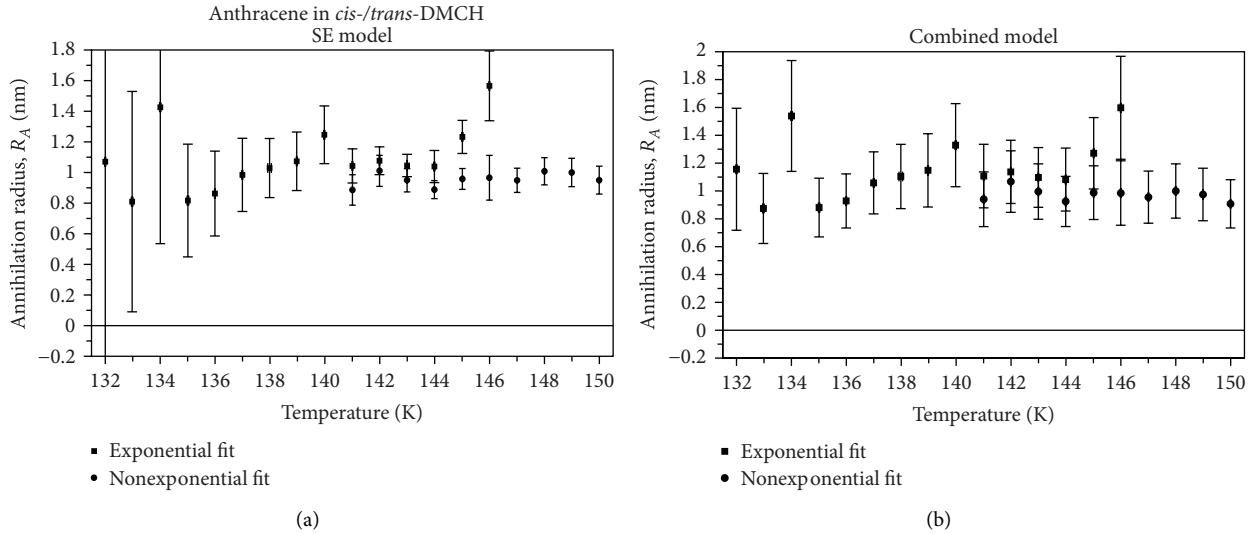

FIGURE 12: The annihilation radius calculated using the values of mutual diffusion coefficient obtained from spatially periodic excitation and different models of temperature and/or viscosity dependence of D_T: (a)—SE model and (b)—combined model. The P_2 parameter was calculated from the non-Fickian model [11] of temporal behavior of the intensity of delayed fluorescence. The plots present the combination of exponential and nonexponential versions of the $I_{DF}(t)$. The experimental data were measured with the short excitation pulse.

results from the screening effect of the first coordination shell which is reproduced in the non-Fickian approach. The other difference is the scattering of the values of the annihilation radius in the range 132 K ÷ 134 K which is not observed in the case of intuitively modified model. At the other side, the values of R_A calculated for P_2 parameter obtained for intuitively modified kinetic model has the tendency to decrease with the decrease of the temperature in the range 132 K ÷ 134 K. In the case of non-Fickian kinetic model this tendency is not observed.

In Figure 13 there is presented the annihilation radius R_A as dependent on the temperature. Here the values were calculated for middle excitation pulse and intuitively modified model of temporal behavior of the intensity of delayed fluorescence. The convention is the same as in the case of Figures 11 and 12. It means: in Figure 13(a) the values of R_A are calculated using the diffusion coefficients from SE model and in Figure 13(b)—from combined model. The course of the annihilation radius as a function of temperature presented in Figure 13 is very similar to that shown in

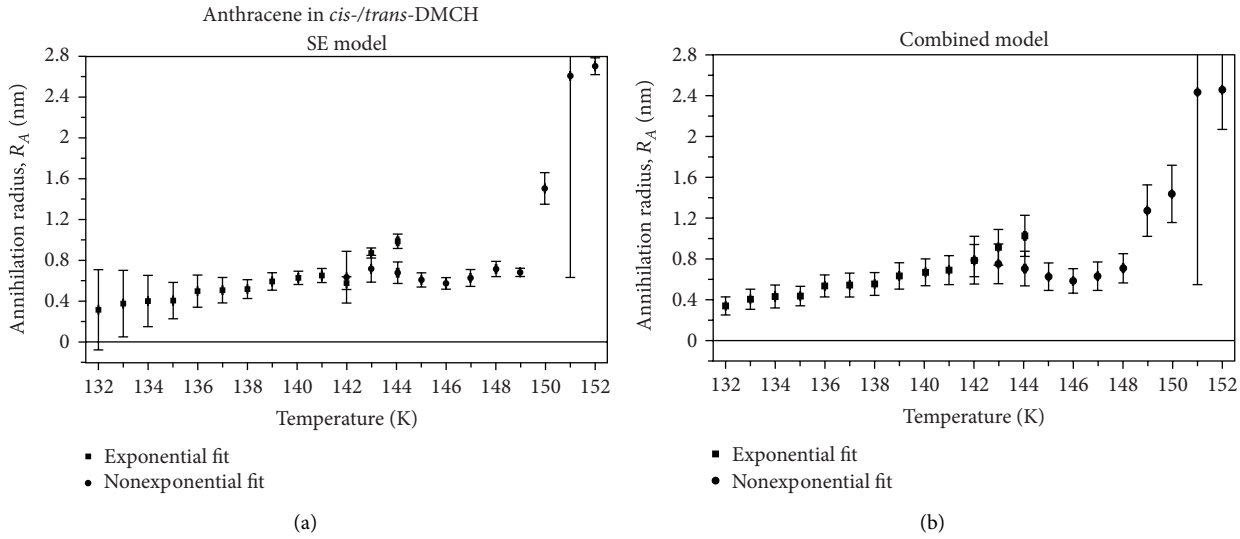

Figure 13: The annihilation radius calculated using the values of mutual diffusion coefficient obtained from spatially periodic excitation and different models of temperature and/or viscosity dependence of D_T: (a) SE model and (b) combined model. The P_2 parameter was calculated from the intuitively modified Smoluchowski model [7] of temporal behavior of the intensity of delayed fluorescence. The plots present the combination of exponential and nonexponential versions of the $I_{DF}(t)$. The experimental data were measured with the middle excitation pulse.

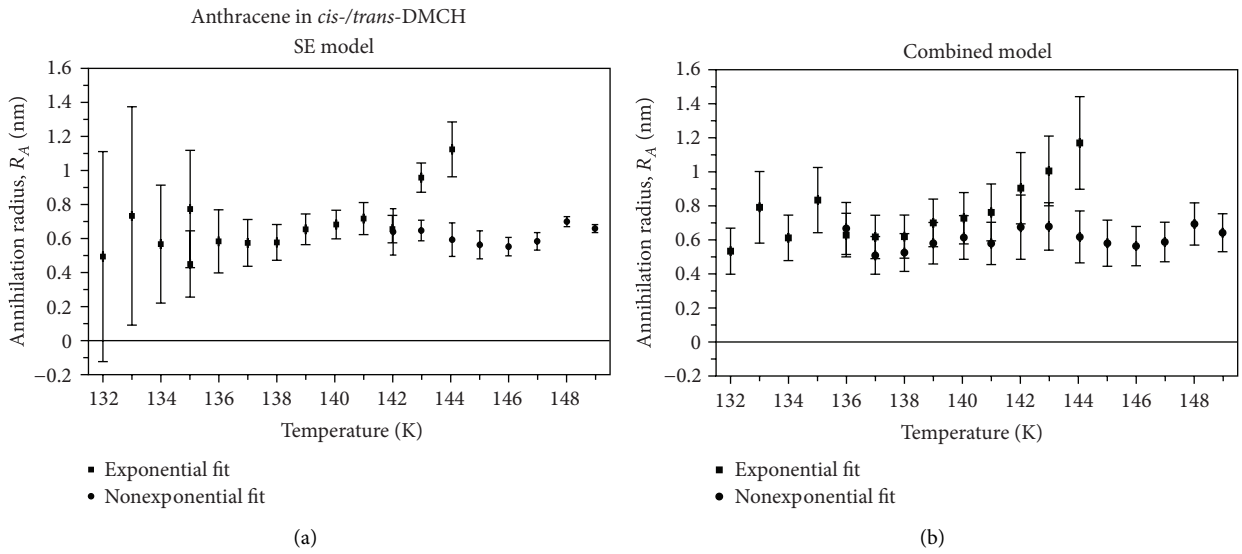

Figure 14: The annihilation radius calculated using the values of mutual diffusion coefficient obtained from spatially periodic excitation and different models of temperature and/or viscosity dependence of D_T: (a) SE model and (b) combined model. The P_2 parameter was calculated from the non-Fickian model [11] of temporal behavior of the intensity of delayed fluorescence. The plots present the combination of exponential and nonexponential versions of the $I_{DF}(t)$. The experimental data were measured with the middle excitation pulse.

Figure 11. The changes of the standard deviation ΔR_A shows the same behavior as a function of temperature for short and middle excitation pulses. It means that the main factor contributing to the accuracy of R_A is the standard deviation of the mutual diffusion coefficient—ΔD_T. Also the average value of R_A in the temperature range where annihilation radius can be treated as constant is for both kind of excitation pulse equal within the accuracy of the measurement and the accuracy of the evaluation procedure.

In Figure 14 there is presented the temperature dependence of R_A in the case of middle excitation pulse and the non-Fickian model of the temporal behavior of the intensity of delayed fluorescence. The convention is the same as in Figures 11, 12, and 13: part (a) presents values of R_A calculated with D_T from SE model and part (b)—with D_T from combined model. The behavior presented in Figure 14 is similar to that one presented in Figure 12 for short excitation pulse. There is only one difference: the average value of R_A

in the temperature range where the annihilation radius can be treated as constant equals to about 0.7 nm for middle excitation pulse. This value is slightly smaller than average R_A for short excitation pulse and the same model of temporal behavior of $I_{DF}(t)$.

5. Concluding Remarks

The introduction of the nonexponential modification to the model describing the temporal behavior of the intensity of delayed fluorescence allowed to enlarge the range of the applicability of the model. In the case exponential model to obtain a good fit one has to perform the experiment in such condition that the measurement of single decay takes very long time (several hours). The measurement of the kinetics of TTA taking long time is extremely difficult because the temperature of the sample must be stabilized within the range of ±0.1 K. Otherwise the fluctuations of viscosity are too large to get reasonable values of parameters. In the case of application of exponential model the mathematical condition: $k_{2A}(t \rightarrow \infty)/k_T < 0.01$ must be satisfied. In the case of nonexponential approach one can obtain good fit for the same parameter equal up to about 0.06. The values of the annihilation radius obtained from nonexponential model are in a good agreement with that from literature and from modified exponential models [7, 11].

It seems that the combined model reproduces quite well the dependence between the diffusion coefficient and the ratio temperature to viscosity over several orders of magnitude. This treatment also removes the artificial upper limit of the diffusion coefficient in SE model: $D_0 \rightarrow \infty$ when $T/\eta \rightarrow \infty$. In the case of very high viscosities application combined or SE model to calculate R_A from intuitively modified Smoluchowski equation results in the decrease of annihilation radius with the decrease of temperature. This kind of decrease of R_A is not observed for the data calculated from non-Fickian kinetic approach. In the case of SE model the increase of ΔR_A with the decrease of the temperature for $T \leq 136$ K is observed. The reason for this behavior is increasing contribution of the uncertainty concerning with the constant factor from (23b).

There are two limits of the discussed model of the kinetics of TTA. First, the nonexponential modifications are based on time-dependent rate parameter $k_{2A}(t)$ from Smoluchowski equation. So in the matter of fact it contains the traces of the time-dependent rate parameter applied for the case of dominant first-order decay [7, 11, 18]. The other limit is concerned with the case of spatially periodic excitation. The evaluation of spatially periodic excited samples is performed as for the spherically symmetric problem, although this irradiation introduces the cylindrical symmetry to the sample which axis is perpendicular to direction of the changes of the intensity of exciting light.

Acknowledgments

The authors thank professor Jürgen Troe (Max-Planck Institute, Göttingen, Germany) for his generous support of the research project. The discussion with professor K. Rotkiewicz (Institute of Physical Chemistry PAS, Warsaw, Poland) was very fruitful for preparation of this paper. The support of stay in Göttingen (Germany) of one of the authors (P. Borowicz) by Max-Planck-Gesellschaft (from October 1, 2000 to September 30, 2001) and by Alexander von Humboldt-Foundation (from October 1, 2001 to December 31, 2002) is gratefully acknowledged. Dr B. Nickel passed away 27/01/2002.

References

[1] P. Avakian and R. E. Merrifield, "Experimental determination of the diffusion length of triplet excitons in anthracene crystals," *Physical Review Letters*, vol. 13, no. 18, pp. 541–543, 1964.

[2] V. Ern, P. Avakian, and R. E. Merrifield, "Diffusion of triplet excitons in anthracene crystals," *Physical Review*, vol. 148, no. 2, pp. 862–867, 1966.

[3] V. Ern, "Anisotropy of triplet exciton diffusion in anthracene," *Physical Review Letters*, vol. 22, no. 8, pp. 343–345, 1969.

[4] B. Nickel, "A modification of the avakian-merrifield method for the determination of the diffusion constant of triplet states," *Berichte der Bunsengesellschaft für Physikalische Chemie*, vol. 76, pp. 582–584, 1972.

[5] B. Nickel and U. Nickel, "The diffusion constant of pyrene molecules in the triplet state in glycerol from −17°C to +15°C," *Berichte der Bunsengesellschaft für Physikalische Chemie*, vol. 76, pp. 584–589, 1972.

[6] E. G. Meyer and B. Nickel, "Diffusion coefficients of aromatic hydrocarbons in their lowest triplet state: anthracene in hexane, octane, hexadecane, perfluorohexane, and methycyclohexane, pyrene and 9, 10-diphenylanthracene in hexane," *Verlag der Zeitschrift für Naturforschung*, vol. 35, pp. 503–520, 1980.

[7] P. Borowicz and B. Nickel, "Application of high-accuracy time-resolved laser spectroscopy to the study of diffusion-controlled triplet-triplet annihilation," *Opto-electronics Review*, vol. 12, no. 3, pp. 325–332, 2004.

[8] J. B. Birks, Ed., *Organic Molecular Photophysics*, vol. 1, Wiley-Interscience, London, UK, 1973.

[9] S. Glasstone, K. J. Laidler, and H. Eyring, Eds., *The Theory of Rate Processes*, McGraw-Hill, New York, NY, USA, 1941.

[10] K. Wirtz, "Kinetische theorie der thermoosmose," *Verlag der Zeitschrift für Naturforschung*, vol. 3, pp. 380–386, 1948.

[11] P. Borowicz and B. Nickel, "Triplet-triplet annihilation in viscous solutions as an example of non-fickian diffusion," *Journal of the Optical Society of America B*, vol. 22, no. 2, pp. 315–322, 2005.

[12] P. Borowicz and B. Nickel, "The kinetics of joined action of triplet-triplet annihilation and first-order decay of molecules in the T1 state in the case of nondominant first-order process," *ISRN Spectroscopy*, vol. 2012, Article ID 316037, 13 pages, 2012.

[13] M. Balucani, V. N. Dobrovolsky, A. V. Osipov, and A. Ferrari, "Model of the drain current saturation in long-gate JFETs and MESFETs," *Solid-State Electronics*, vol. 49, no. 8, pp. 1251–1254, 2005.

[14] M. Bellodi and J. A. Martino, "Study of the leakage drain current carriers in silicon-on-insulator MOSFETs at high temperatures," *Solid-State Electronics*, vol. 45, no. 5, pp. 683–688, 2001.

[15] C. J. Sheu and S. L. Jang, "Modeling of electron gate current and post-stress drain current of p-type silicon-on-insulator

MOSFETs," *Solid-State Electronics*, vol. 47, no. 4, pp. 705–711, 2003.

[16] A. Christou, "Charge transport in low-dimensional nitride semiconductor heterostructures," *Physica B*, vol. 296, no. 1–3, pp. 264–270, 2001.

[17] N. Karl, "Charge carrier transport in organic semiconductors," *Synthetic Metals*, vol. 133-134, pp. 649–657, 2003.

[18] B. Nickel, P. Borowicz, A. A. Ruth, and J. Troe, "Application of Smoluchowski's generalized theory to the kinetics of triplet-triplet annihilation of anthracene in viscous solution after long-pulse excitation," *Physical Chemistry Chemical Physics*, vol. 6, no. 13, pp. 3350–3363, 2004.

[19] B. Nickel, H. E. Wilhelm, and C. P. Jaensch, "Effect of the Förster energy transfers $S_1 + S_3 \rightarrow S_0 + S_n$ and $S_1 + T_1 \rightarrow S_0 + T_n$ on the time dependence of the delayed fluorescence from aromatic compounds: anti-Smoluchowski and Smoluchowski temporal behavior," *Optika i Spektroskopiya*, vol. 83, no. 4, pp. 541–556, 1997.

[20] J. Jasny, B. Nickel, and P. Borowicz, "Wavelength- and temperature-dependent measurement of refractive indices," *Journal of the Optical Society of America B*, vol. 21, no. 4, pp. 729–738, 2004.